

## Ovine Forestomach Matrix (OFM) Stimulates Angiogenesis *In Vitro* and *In Vivo*

Sharleen M. Irvine<sup>1,2</sup>, Juliet Cayzer<sup>1</sup>, Elise M. Todd<sup>1</sup>, Stan Lunj<sup>1</sup>, Evan W. Floden<sup>1</sup>, Leonardo Negroni<sup>1</sup>, James N. Fisher<sup>1</sup>, Sandi G. Dempsey<sup>1</sup>, Alan Alexander<sup>1</sup>, Michael C. Hill<sup>1</sup>, Annaliese O'Rourke<sup>1</sup>, Sarah P. Gunningham<sup>1</sup>, Cameron Knight<sup>1</sup>, Paul F. Davis<sup>1</sup>, Brian R. Ward<sup>1</sup>, Barnaby C.H. May<sup>1</sup>

<sup>1</sup>Mesynthes Limited, 69 Gracefield Road, Lower Hutt 5040, New Zealand

<sup>2</sup>Department of Medicine, University of Otago, Wellington, New Zealand, <sup>3</sup>Estadart Limited, Palmerston North, New Zealand,

<sup>4</sup>Waikato District Health Board, Hamilton, New Zealand, <sup>5</sup>Trinity Bioactives Limited, Lower Hutt, New Zealand,

<sup>6</sup>Angiogenesis and Cancer Research Group, University of Otago, Christchurch, New Zealand, <sup>7</sup>Institute of Veterinary, Animal and Biomedical Sciences, Palmerston North, New Zealand

### Abstract



Extracellular matrix (ECM)-based biomaterials have an established place as medical devices for wound healing and tissue regeneration. In the search for biomaterials we have produced ovine forestomach matrix (OFM), an ECM which is biochemically diverse and biologically functional. OFM was shown to retain residual basement membrane components, such as laminin and collagen IV and a collagenous microarchitecture comprised of fibronectin, glycosaminoglycans, and elastin. OFM is shown to retain bioactive factors such as fibroblast growth factor 2 (FGF2) using a pheochromocytoma cell (PC12) model of differentiation. OFM was non-toxic to mammalian cells and supported fibroblast and keratinocyte migration, differentiation and infiltration. OFM stimulated endothelial cell migration in a HUVEC wound scratch assay and increased microvasculature in an aortic ring model. Blood vessel area and vascular sprouting increased in response to OFM in an ex vivo chicken chorioallantoic membrane (CAM) assay. The OFM biomaterial was shown to undergo remodelling in a porcine full thickness excisional model and gave rise to significantly more blood vessels than small intestinal submucosa (SIS)-treated or untreated wounds. The ability of OFM to encourage blood vessel growth and angiogenesis is a property that lends itself well to clinical applications in wound healing and tissue regeneration.

### OFM Biochemical Composition

The major and minor biochemical components of OFM were quantified using established techniques. OFM was shown to be a rich biological matrix containing connective, adhesion and signaling proteins, all of which play critical roles in cell adhesion as well as differentiation and proliferation (Figure 1). The matrix was composed mainly of collagen, including types I and III. Structural ECM components included elastin and fibronectin and sulphated GAGs. Proteins important in cell adhesion and infiltration such as laminin and collagen IV were detected. ECM-associated molecules including signalling proteins such as FGF2 and hyaluronic acid.

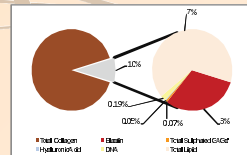


Figure 1. Major biochemical composition OFM.

### OFM Supports Cellular Infiltration

Human fibroblasts (D551) were seeded onto hydrated OFM and cultured for up to 10 days with fresh media being added every other day. OFM was formalin fixed, sectioned and stained with DAPI then visualized using fluorescent microscopy. Fibroblasts were seen to have infiltrated into the OFM within 12 hours post-seeding (Figure 2A) and extensive infiltration could be observed after 10 days (Figure 2C).

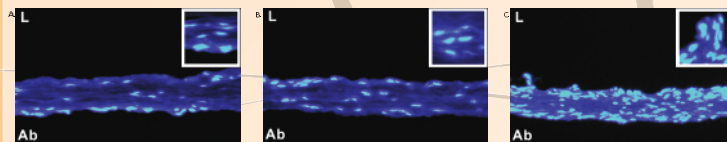


Figure 2. Representative images of DAPI stained OFM infiltrated with human fibroblasts after 0.5 days (A), 5 days (B) and 10 days (C). Cells were seeded to the abdominal surface and images have been rotated to maintain the relevant orientation of the OFM. 20x magnification, with 40x magnification insets. Luminal and abdominal surfaces are indicated with 'L' and 'A' respectively.

### OFM Stimulates Cell Differentiation via Bioactive FGF2

To explore the stimulatory activity of OFM on mammalian cells as a result of bioactive FGF2, studies were conducted using pheochromocytoma cells of the rat adrenal medulla (PC12). PC12 cells were exposed to OFM extracted into basal media, and the cellular differentiation was quantified. In the presence of bioactive growth factors, PC12 will differentiate i.e. sprout neuronal processes (Figure 3A). Untreated cells exhibited no differentiation (Figure 3B) yet OFM extracts promoted cell differentiation (Figure 3C) in a dose dependent manner (Figure 3D).

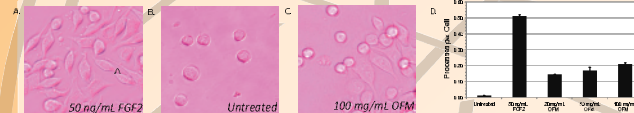


Figure 3. Representative images of PC12 cells treated with 50 ng/ml, 100 ng/ml, and 1000 ng/ml OFM extract. (A) and (B) are treated with OFM extract at 100 ng/ml protein concentration. (C) 40x magnification. Quantification of neuronal differentiation in the presence of OFM extract. Concentration only indicated are the 50 ng/ml protein concentration of OFM extract in culture. Error bars represent SEM from three independent experiments.

To examine the effect of bioactive FGF2 on PC12 differentiation, FGF2 activity was blocked using an anti-FGF2 antibody (Figure 4A). Cell differentiation was partially inhibited (Figure 4B) by the anti-FGF2 antibody, demonstrating that FGF2 was present in a bioactive form.

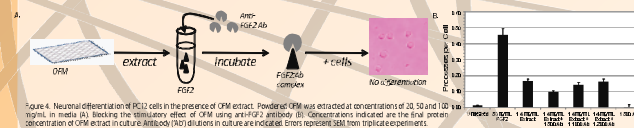


Figure 4. Neuronal differentiation of PC12 cells in the presence of OFM extract. Purified OFM was extracted at concentrations of 20, 50 and 100 ng/ml. In media (A). Blocking the stimulatory effect of OFM using anti-FGF2 antibody (B). Differentiation indicated are the final protein concentration of OFM extract in culture. Antibody (100) dilutions in culture are indicated. Error bars represent SEM from triplicate experiments.

### OFM Stimulates Angiogenesis *In Vitro*

The rat aortic ring model is an established assay for quantifying angiogenesis *in vitro*. A fibrin clot was prepared either as a OFM suspension or an OFM extract and used to surround a freshly harvested rat aortic ring. Aortic rings were imaged at days 0, 3, 5 and 7, and the extent of vascularization was visualized using Image J (Figures 5B, 5D). Microvasculature extending from OFM-treated rings (Figure 5C) was significantly increased relative to the untreated control (Figure 5E).

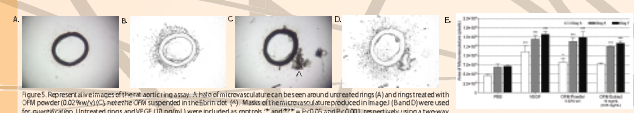


Figure 5. Representative images of aortic rings in a assay. A left of microvasculature seen between and around untreated rings (A) and rings treated with OFM extract (200 ng/ml) relative to OFM suspended in fibrin (B). (C) Microvasculature extending from OFM-treated rings (C) and untreated rings (A) and rings treated with OFM extract (200 ng/ml) relative to OFM suspended in fibrin (B). (D) Quantification of microvasculature extending from OFM-treated rings (C) and untreated rings (A) and rings treated with OFM extract (200 ng/ml) relative to OFM suspended in fibrin (B). Error bars represent SEM from triplicate experiments. \*P<0.05 and \*\*P<0.01 respectively using a two-way ANOVA with Bonferroni post-hoc tests relative to untreated controls.

The HUVEC wound scratch assay is an established assay for assessing endothelial migration and proliferation. HUVEC monolayers were scratched using a pipette tip, and extracts of OFM, SIS, cross-linked OFM (OFM-X) and Promogran® (PG) in media were added to the monolayer then scratches were imaged at 0 h, 4 h and 8 h. OFM-treated cells showed greater cellular infill relative to untreated controls in the absence of mitomycin C (Figure 6A, B). The extent of cellular migration alone was then assessed by arresting proliferation. OFM-treated wells (Figure 6C, D) demonstrated significant increases in migration relative to untreated controls (Figure 6A, B) and compared to SIS, OFM-X and PG (Figure 6E).



Figure 6. Representative images of HUVEC proliferation and migration (A, B) and migration only (C, D) in response to either PBS (A, C) or OFM extract (B, D). Magnification of the monolayer at 4h is depicted as a black line whereas magnification at 8h is indicated by the white line. Quantification of the change in size of cells (proliferation) measured by migration alone relative to 4h (B, D). Concentration indicated in brackets is the protein concentration of the extract (100 ng/ml media). Error bars represent SEM from triplicate experiments. \*P<0.05, \*\*P<0.01 and \*\*\*P<0.001 respectively, using a two-way ANOVA and Bonferroni post-hoc tests relative to the untreated controls.

### OFM Stimulates Angiogenesis *Ex Ovo*

The *ex ovo* chick CAM assay is an established assay for quantifying angiogenesis *in vivo*. Fertilised eggs were incubated (38.5 °C) for 3 days before being cracked into a petri dish and incubated at 37.5 °C for 3 days. PBS extracts of OFM, SIS, OFM-X and PG were added onto the developing vessels of the CAM. Each dose site was photographed at 24 h, 48 h and 72 h post-dosing and the vascular area and branchpoint numbers were quantified. OFM-treated CAM showed increases in both vascular area (Figure 7D) and branchpoint number (+/- Figure 7C) compared to PBS controls (Figure 7A, B). OFM-treated sites showed significantly higher vascular area (Figure 7D) than SIS, OFM-X and PG (P<0.01) as well as significant increases in branchpoint number at all time points (data not shown).

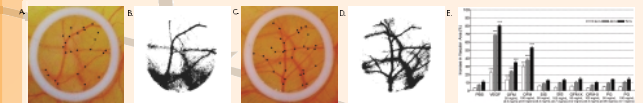


Figure 7. Representative images of the CAM assay following treatment with OFM extract (100 mg/ml) day 0 (A). Black dots indicate position of branchpoints for branchpoint analysis. Masks of the blood vessels produced in image (B and C). Representative images of the CAM assay following treatment with OFM extract (100 mg/ml) day 3 (C). Quantification of the percentage increase in the total blood vessel area, relative to PBS (D). Error bars represent standard error from triplicate experiments. \*P<0.05 and \*\*P<0.01 respectively, using a two-way ANOVA and Bonferroni post-hoc tests relative to the untreated controls.

### OFM Stimulates Remodeling and Angiogenesis *In Vivo*

In order to evaluate the *in vivo* tolerance of OFM and determine its ability to stimulate tissue regeneration and to undergo remodelling, we conducted a comprehensive wound healing study in pigs. On day 0 of the study, a total of 20 full thickness 20 mm diameter wounds were surgically created on the back of a 6 week old anesthetized female pig (approx. 18-20 kg) using a dermal punch. Each of the wounds were either untreated, or treated with sterile OFM or SIS. On days 0, 3, 7, 14, 28 and 42 all wounds were digitally imaged (Figure 8) and a single row of wounds from each animal was biopsied under anesthesia. All biopsies were formalin fixed, mounted, sectioned and stained for analysis.

Figure 8. Representative images of porcine full thickness excisional wounds at day 0 before treating with OFM (A) and Day 42, after treatment with OFM (B).

### Remodeling

An examination of Gomori's trichrome stained tissue biopsies taken during the course of the study provided evidence that OFM was infiltrated by cells during the healing process (Figure 9). OFM appeared as green ribbons especially prominent at day 7. Cells were clearly visible within the exogenous ECM collagen scaffold at day 7. Both OFM and SIS were visible for approximately 14-28 days, after which time mature collagen had been laid down and the matrices were not visible within the wound bed. A variety of immune cells were observed within and surrounding the matrices and this immune response had resolved by day 42.

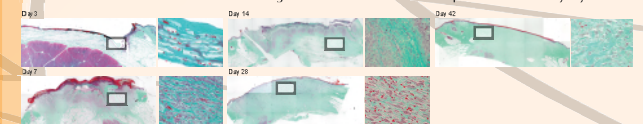


Figure 9. Representative images of Gomori's trichrome stained tissue biopsies from OFM treated wounds. Wounds were biopsied on days as indicated above and slices were stained and imaged at 4x then extracted to generate a whole wound image (see caption). Green: collagen and blue: nuclei. Higher magnifications (40x) are taken within the area of the 4x image outlined.

### Angiogenesis

Sections were stained with anti-CD34 antibody, labelled with DAB and the vasculature quantified. There was a statistically significant increase in the number of blood vessels in wounds treated with OFM (Figure 10A), relative to untreated wounds (Figure 10B). The average total number of vessels counted per frame is given in Figure 10C. The increase in total blood vessels was evident on days 14, 28 and 42 (P<0.01). In comparison, SIS-treated wounds showed no significant increase in blood vessels relative to the untreated control.

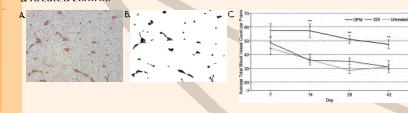


Figure 10. Representative image of a CD34 stained tissue section (A). The same image split into a H&E mask using ImageJ where blood vessels appear black and are counted accordingly (B). Average total number of blood vessels counted per frame, analysed for each tissue biopsy (C). Error bars represent SEM from the 20 biopsies analysed for each treatment group. \*P<0.05 and \*\*P<0.01 significance relative to untreated control using a two-way ANOVA.